





Mapping proteome-wide targets of protein kinases in plant stress responses

Pengcheng Wang^{a,1,2} , Chuan-Chih Hsu^{b,1} , Yanyan Du^{a,b,1}, Peipei Zhu^c, Chunzhao Zhao^{a,d}, Xing Fu^a, Chunguang Zhang^d, Juan Sebastian Paez^b, Alberto P. Macho^a , W. Andy Tao^{b,c,2}, and Jian-Kang Zhu^{a,b,d,2} 

^aShanghai Center for Plant Stress Biology, CAS Center for Excellence in Molecular Plant Sciences, Chinese Academy of Sciences, 200032 Shanghai, China; ^bDepartment of Biochemistry, Purdue University, West Lafayette, IN 47907; ^cDepartment of Chemistry, Purdue University, West Lafayette, IN 47907; and ^dDepartment of Horticulture and Landscape Architecture, Purdue University, West Lafayette, IN 47907

Contributed by Jian-Kang Zhu, December 13, 2019 (sent for review November 13, 2019; reviewed by Heribert Hirt and Shuqun Zhang)

Protein kinases are major regulatory components in almost all cellular processes in eukaryotic cells. By adding phosphate groups, protein kinases regulate the activity, localization, protein–protein interactions, and other features of their target proteins. It is known that protein kinases are central components in plant responses to environmental stresses such as drought, high salinity, cold, and pathogen attack. However, only a few targets of these protein kinases have been identified. Moreover, how these protein kinases regulate downstream biological processes and mediate stress responses is still largely unknown. In this study, we introduce a strategy based on isotope-labeled in vitro phosphorylation reactions using in vivo phosphorylated peptides as substrate pools and apply this strategy to identify putative substrates of nine protein kinases that function in plant abiotic and biotic stress responses. As a result, we identified more than 5,000 putative target sites of osmotic stress-activated SnRK2.4 and SnRK2.6, abscisic acid-activated protein kinases SnRK2.6 and casein kinase 1-like 2 (CKL2), elicitor-activated protein kinase CDPK11 and MPK6, cold-activated protein kinase MPK6, H₂O₂-activated protein kinase OX11 and MPK6, and salt-induced protein kinase SOS1 and MPK6, as well as the low-potassium-activated protein kinase CIPK23. These results provide comprehensive information on the role of these protein kinases in the control of cellular activities and could be a valuable resource for further studies on the mechanisms underlying plant responses to environmental stresses.

phosphorylation | substrate | cold stress | salt stress | oxidative stress

Eukaryotic protein kinases are major regulatory components for various cellular functions. By adding phosphate groups to substrate proteins, protein kinases control the activity, localization, association with other proteins, and overall function of many proteins and thereby regulate almost all cellular processes. Compared to other eukaryotes, flowering plants have more genes encoding protein kinases in their genomes. In the model plant *Arabidopsis thaliana*, more than 1,000 protein kinases (1) and 20,000 phosphosites (2) have been identified.

Mitogen-activated protein kinase (MAPK) cascades play pivotal roles in the regulation of plant responses to both environmental changes and pathogen attack (3–5). Activation of MAPKs is one of the earliest signaling events after plant sensing of pathogen/microbe-associated molecular patterns and pathogen effectors (4, 6) and is essential for the activation of immune responses. MPK3 and MPK6 are well-studied pathogen-responsive MAPKs, and several of their protein substrates have been identified (4, 6). These substrates contribute to the biosynthesis of plant stress/defense hormones and subsequent signaling, generation of reactive oxygen species, activation of defense-related genes, phytoalexin biosynthesis, and hypersensitive response-associated cell death (4). In addition to MPK3/6, several calcium-dependent protein kinases (CDPKs/CPKs), namely CPK4, CPK5, CPK6, and CPK11, contribute to plant immune signaling (7).

It is well known that protein kinases are central components in the response of plants to abiotic stresses (8). Sucrose nonfermenting

(SNF1)-related protein kinase 2s (SnRK2s) are central components in plant responses to drought and osmotic stresses. There are 10 members in the SnRK2 family in *Arabidopsis* (SnRK2.1 to SnRK2.10) and rice (SAPK1 to SAPK10). In *Arabidopsis*, three of them, SnRK2.2, SnRK2.3, and SnRK2.6, are activated by abscisic acid (ABA), a phytohormone important for plant responses to several abiotic stresses (9), and play critical roles in ABA responses (10, 11). Moreover, all SnRK2s except SnRK2.9 can be activated by osmotic stress caused by NaCl or mannitol treatment in *Arabidopsis* (12, 13). In addition to SnRK2s, CPKs are also important for ABA signaling (14). Several other kinases, such as calcineurin B-like protein interacting serine/threonine-protein kinase 23 (CIPK23) and casein kinase 1-like 2 (CKL2), are essential for ABA-induced stomatal closure and drought resistance (15–18), and SALT OVERLY SENSITIVE 2 (SOS2), also known as CIPK24, is a key regulator of salinity response in plants (19). High salinity increases the cytosolic calcium content, which is sensed by the calcium sensor SOS3 (calcineurin B-like calcium sensor protein 4/CBL4) in roots (19), and by SCaBP8/CBL10 in shoots (20).

Significance

Despite the importance of phosphorylation-dependent signaling for cellular physiology, identification of kinase substrates remains very challenging. In this study, we developed an approach that uses natural phosphopeptides as the substrate pool to identify peptides that can be phosphorylated in vitro, which correspond to putative direct targets of the tested protein kinases. Our results demonstrate the simplicity, sensitivity, and reproducibility of this approach. By identifying more than 5,000 putative kinase–substrate pairs, our study reveals an unprecedented proteome-wide map of the targets of protein kinases during plant stress responses, which provides comprehensive information on the role of these kinases in controlling cellular activities and constitutes a valuable resource for the community.

Author contributions: P.W., C.-C.H., W.A.T., and J.-K.Z. designed research; P.W., C.-C.H., Y.D., P.Z., C. Zhao, and C. Zhang performed research; P.W., C.-C.H., Y.D., X.F., J.S.P., and J.-K.Z. analyzed data; and P.W., C.-C.H., A.P.M., W.A.T., and J.-K.Z. wrote the paper.

Reviewers: H.H., King Abdullah University of Science and Technology; and S.Z., University of Missouri.

The authors declare no competing interest.

Published under the PNAS license.

Data deposition: All mass spectrometric data have been deposited to the ProteomeXchange Consortium via the PRIDE partner repository (<https://www.ebi.ac.uk/pride/archive/>) with the dataset identifier PXD010053. All of the results from the in vivo and in vitro proteomics in this study can be accessed online via our protein kinase–substrate database (KSDB, <http://ksdb.psc.ac.cn>).

¹P.W., C.-C.H., and Y.D. contributed equally to this work.

²To whom correspondence may be addressed. Email: pcwang@sibs.ac.cn, watao@purdue.edu, or jkzhu@sibs.ac.cn.

This article contains supporting information online at <https://www.pnas.org/lookup/suppl/doi:10.1073/pnas.1919901117/-DCSupplemental>.

First published January 28, 2020.

SOS3 and CBL10 activate SOS2, and SOS2 then phosphorylates and activates the plasma membrane Na^+/H^+ antiporter SOS1 (21). SOS1 is the only known substrate of SOS2 thus far, and how SOS3-SOS2 regulates salinity responses is not fully understood.

Despite the importance of phosphorylation-dependent signaling for cellular physiology, the identification of kinase substrates, which is essential for understanding the role of the kinases in signaling pathways, is still very challenging. Protein arrays have been used to identify kinase substrates using purified protein kinases and radiolabeled adenosine triphosphate (ATP) (22, 23), and global phosphorylation networks in yeast and MAP kinase modules in *Arabidopsis* were studied using protein array-based methods (23, 24). Peptide arrays with synthetic peptides were also used to study the specificity and activity of protein kinases (25, 26). Kinase assays with ATP analog (N^6 -benzyl-ATP) and analog-sensitive protein kinase isoforms were used to determine the substrates of several protein kinases (27–29), although these approaches can only be used to study certain kinases in which an analog-sensitive mutation does not affect kinase activity. Phosphoproteomics provides a powerful tool to study the signaling network of protein kinases and has been applied to the identification of downstream effectors of mammalian target of rapamycin (30) and ABA-activated SnRK2s targets in *Arabidopsis* (31, 32). However, these phosphoproteomics methods cannot distinguish between direct substrates and indirect downstream effectors and often fail to detect low-abundance phosphosites.

To systematically identify the direct substrates of protein kinases with high confidence, we developed a kinase assay linked phosphoproteomics (KALIP) approach by coupling an in vitro kinase assay-based substrate screening with in vivo kinase-dependent phosphoproteomic analysis (33, 34). Although KALIP is a straightforward method to identify putative direct targets, it requires large-scale phosphoproteomic experiments involving fractionations due to the high complexity of phosphoproteomes and the low abundance of many kinase substrates. To take advantage of the KALIP approach and overcome its limitations, we have significantly improved the KALIP approach to allow for a high-throughput identification of kinase substrates, using one single mass spectrometry (MS) analysis for each kinase. This strategy is based on isotope-labeled in vitro phosphorylation reactions using in vivo phosphorylated peptides as kinase substrate pools, and our use of enriched phosphoproteomes substantially reduces the complexity of substrate pools. Moreover, stable isotope-labeled ATP is used as ATP donor to avoid the interference from background phosphorylation, and a two-step phosphopeptide-enrichment workflow is used to increase sensitivity. We demonstrate the simplicity, sensitivity, and reproducibility of this approach by identifying MAPK substrates as a proof of concept and further applied this approach to profile the putative substrates of several plant kinases that play critical roles in the regulation of plant responses to environmental stresses. Using this method, 5,075 putative targets of nine protein kinases were identified. Several of these substrates were validated by traditional in vitro assays using recombinant proteins, confirming the reliability of this approach. These results provide comprehensive information on the role of these protein kinases in controlling cellular activities and advance our understanding of plant responses to biotic and abiotic stresses. Moreover, this work paves the way for the application of similar strategies to the study of phosphorylation networks mediated by other protein kinases.

Results and Discussion

Development of the KALIP 2.0 Method and Identification of MPK6 Substrates. We aimed at developing a high-throughput KALIP-based approach with improved sensitivity, specificity, and reproducibility. This requires 1) a simple and targeted substrate pool for the in vitro kinase assay, 2) high reproducibility of the kinase reaction for label-free quantification, and 3) good correlation

between in vitro and in vivo results. To this end, we developed a strategy integrating a stable isotope-labeled in vitro kinase assay, using enriched phosphopeptides as the substrate pool, together with quantitative measurements, termed KALIP 2.0. The workflow of this approach is depicted in Fig. 1. Proteins extracted from plant samples are first digested with Lys-C to generate long peptide fragments that retain the phosphorylation motif in the peptides (e.g., $[-\text{R}-\text{x}-\text{x}-(\text{pS}/\text{pT})-]$). The Lys-C-digested phosphopeptides from either mock or stress-treated *Arabidopsis* seedlings are then enriched using polymer-based metal ion affinity capture (polyMAC). The enriched phosphopeptides are treated with alkaline phosphatase to remove preexisting phosphorylation, and the dephosphorylated peptides are then subjected to a kinase reaction with a recombinant protein kinase and heavy isotope ^{18}O -ATP as phosphate donor. The heavy phosphate-labeled peptides are further digested with trypsin and enriched again using polyMAC. The purified heavy phosphopeptides are finally analyzed by liquid chromatography coupled to tandem MS (LC-MS/MS). On the one hand, the use of in vivo-phosphorylated peptides as substrate pool for in vitro kinase reactions greatly reduces the complexity of the substrate pool and allows for the identification of low-abundance targets; on the other, it ensures that the identified phosphorylation events are more likely to exist *in planta*.

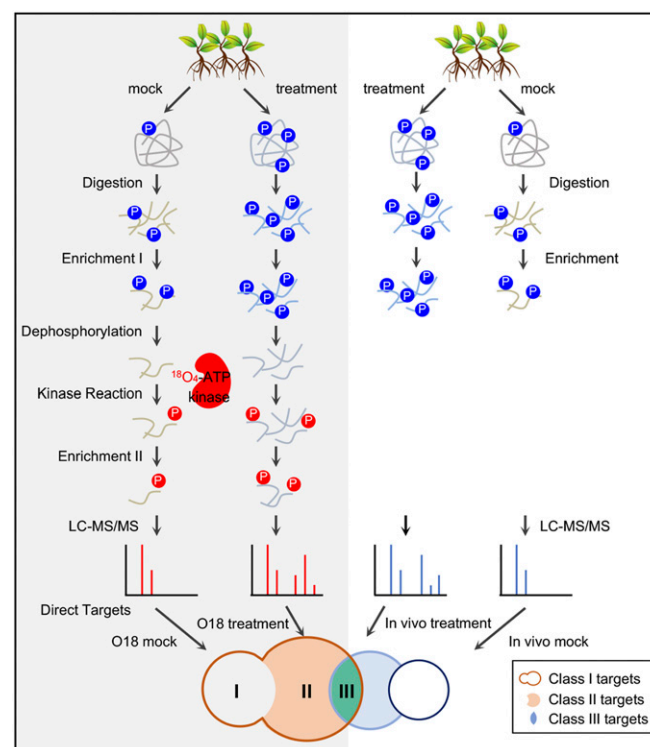


Fig. 1. The KALIP 2.0 workflow for identifying kinase substrate proteins. Protein extracts from mock- and stress-treated seedlings were digested with Lys-C, and the resulting long phosphopeptides (blue) were enriched by polyMAC. The phosphopeptides were dephosphorylated and incubated with a recombinant kinase and $\gamma\text{-}^{18}\text{O}_4\text{-ATP}$, and ^{18}O -phosphate-labeled peptides (red) were enriched again through polyMAC and analyzed by LC-MS/MS. Proteins with heavy (^{18}O) phosphopeptides identified from all samples were classified as class I substrates (red circle). The phosphoproteins with heavy phosphosites significantly enriched in the stress-activated samples ($\text{FDR} < 0.05$) were classified as class II substrates (orange). Phosphoproteins significantly enriched in stress-treated samples in both the in vitro kinase reaction and in vivo kinase-dependent phosphoproteomic comparison were classified as class III substrates (green).

We compared the performance of KALIP 2.0 with our previous KALIP approaches that use either the entire digested peptides (KALIP-peptide) (33) or extracted proteins (KALIP-protein) (34) as the kinase substrate pool. The workflow of the three approaches is represented in *SI Appendix, Fig. S1A*. We used recombinant MPK6 protein preactivated by its upstream activator MKK5^{DD} as kinase and samples from *Arabidopsis* seedlings treated with flg22 (an immune-elicitor peptide from bacterial flagellin) as substrate pool. MPK6 is a well-studied protein kinase, which is activated in response to cold, oxidative, and biotic stresses (35–38). A total of 158, 280, and 1,588 unique ¹⁸O-phosphopeptides were identified from flg22-treated seedlings using KALIP-protein, KALIP-peptide, and KALIP 2.0, respectively (*Fig. S1 B–D* and *Dataset S1*). The KALIP 2.0 strategy identified many more ¹⁸O-phosphopeptides compared to the KALIP-protein and KALIP-peptide strategies, suggesting that the use of enriched phosphopeptides as the substrate pool greatly reduced the complexity of the substrate pool and thus increased the detection of many low-abundance substrates. Next, we compared the number of phosphopeptides overlapping between the in vitro ¹⁸O-phosphopeptides from the three strategies and in vivo phosphoproteomics data. A total of 83, 65, and 845 identified ¹⁸O-phosphopeptide sequences from the KALIP-protein, KALIP-peptide, and KALIP 2.0 strategies were present among the in vivo flg22-activated phosphopeptides, respectively (*SI Appendix, Fig. S1 B–D*). This comparison shows that KALIP 2.0 is 10 and 13 times more efficient than the KALIP-protein and KALIP-peptide approaches, respectively, at identifying MPK6-phosphorylated peptides present among the in vivo flg22-activated phosphopeptides, supporting that enriching phosphopeptides prior to the MPK6 reaction greatly improves the sensitivity of the approach.

Upon application of this strategy, we categorized the putative direct substrates of the investigated kinases into three subgroups (*Fig. 1*): phosphoproteins with heavy phosphosites identified in all samples were classified as class I substrates, which include all possible direct targets of MPK6; phosphoproteins with heavy phosphosites significantly enriched in the stress-activated samples (false discovery rate [FDR] < 0.05) were classified as class II substrates, which can be considered as putative direct targets that specifically respond to the stress; the class II substrates were also compared with the in vivo phosphoproteomics results, and the phosphoproteins significantly enriched in both the in vitro kinase assay and in vivo kinase-dependent phosphoproteomic datasets (FDR < 0.05) were classified as class III substrates. Compared to class I and class II, class III substrates are more likely to be in vivo relevant substrates. This classification helps to minimize false positive hits and nonspecific substrates and allow for the selection of appropriate candidate substrates to perform further biochemical validation or functional analysis.

Recombinant, preactivated MPK6 protein was utilized to phosphorylate the dephosphorylated peptides of cold- and H₂O₂-treated phosphoproteomes, in addition to the flg22-treated phosphoproteome. As a result, 4,873 phosphopeptides, representing 1,974 unique phosphoproteins, were identified as putative MPK6 substrates (class I) from flg22-treated samples (*Dataset S2*); 4,823 phosphopeptides, representing 1,970 unique phosphoproteins, and 4,939 phosphopeptides, representing 1,923 unique phosphoproteins, were identified as putative MPK6 substrates from H₂O₂- and cold-treated samples, respectively (*Datasets S3 and S4*).

To analyze the reproducibility of this kinase–substrate screening approach, we calculated the Pearson correlation coefficients between the three replicates of each sample and visualized the class I putative targets using heat maps (*SI Appendix, Fig. S2A*). The Pearson correlation coefficients were greater than 0.9 among all replicates of each sample, confirming the robustness of this approach for quantitative comparison. To assess the similarities and differences of the four samples, a principal component analysis (PCA) was performed. Component 1 clearly separates the stress-

induced MPK6 substrates (cold, H₂O₂, and flg22) from the MPK6 substrates in mock-treated samples, suggesting that stress conditions significantly modulate the kinase activity of MPK6 in vivo (*Fig. 2A*). Component 2 shows the segregation of different stress-triggered substrates. There is a distinct separation of the cold-activated MPK6 substrates and a moderate segregation of H₂O₂- and flg22-induced MPK6 substrates. These results indicate that using stress-induced phosphoproteomes as kinase–substrate pools makes it possible to distinguish distinct stress-induced substrates.

Furthermore, 16 of 34 previously reported MPK substrates with biochemical and genetic evidence were identified by KALIP 2.0 (*Fig. 2B*). We also compared our list of putative MPK6 substrates with previous high-throughput studies on MPK6 substrates (*Fig. 2C*). Our data included 26 out of 32 and 37 out of 52 putative MPK3/6 substrates identified by two previous phosphoproteomic studies, respectively (39, 40); 5 out of 56 and 18 out of 184 putative MPK3/6 substrates identified by two protein array-based studies were also present in our list of MPK6 targets, respectively (24, 41). In contrast, there were no or very few overlaps among these previous lists of putative substrates (*Fig. 2C*).

Besides the previously reported substrates, we identified more than 2,000 additional putative substrates of MPK6 (*Datasets S2–S4*) using KALIP 2.0. We performed unsupervised hierarchical clustering of the 950 heavy phosphosites (class II) with significant differences among the three stresses (FDR < 0.05) to highlight differential phosphoproteins identified in unique stress conditions (*Fig. 2D*). The heat map revealed four main clusters of proteins differentially represented in the three stress-treated samples. Cluster 1 contains the phosphosites enriched in H₂O₂- and cold-treated MPK6 substrates but not changed by flg22 treatment. Cluster 2 contains MPK6 substrates significantly enriched only in H₂O₂-stimulated samples. Cluster 3 shows the proteins with phosphosites enriched in MPK6 substrates in cold- and flg22-treated samples but not in H₂O₂-treated samples. Cluster 4 shows the proteins with phosphosites significantly enriched in MPK6 substrates in flg22-treated samples. Gene Ontology (GO) analysis showed that cluster 4 shows a high prevalence of MPK6 substrates that are involved in organelle relocation. Cluster 2, which contains MPK6 substrates in H₂O₂-activated samples, shows an overrepresentation of proteins that mediate mRNA metabolic process and RNA processing, suggesting that MPK6 regulates gene expression through modulation of RNA metabolism under H₂O₂ treatment. Cluster 3 shows an overrepresentation of proteins that modulate substance transportation under cold and flg22 treatments, including vesicle-mediated transport, intracellular transport, and response to inorganic substance. These results suggest that our approach using a stress-perturbed phosphoproteome as the kinase–substrate pool enables a highly reproducible and selective identification of substrates unique to different stress conditions.

To test if the identified putative substrates could serve as substrates of MPK6 in vitro, several target proteins were randomly selected, expressed, and purified from *Escherichia coli* and tested in kinase assays in vitro. Five out of seven of the tested proteins, uridine diphosphate (UDP)-xylose synthase 5 (UXS5, class III), GTPase-activating protein (GAP) for Ypt family protein (gyp1p, class III), companion of cellulose synthase (CC3, class I), MAP65-1 (class III), villin 3 (VLN3, class II), and mechanosensitive channel of small conductance-like 9 (MSL9, class II), showed strong phosphorylation signals, while the other two, AT1G62480 (class III) and member of the latex protein (MLP)-like protein 423 (MLP423, class III), showed relatively weak signals (*Fig. 2E*). The results support that our KALIP 2.0 method is efficient for the identification of direct protein kinase substrates.

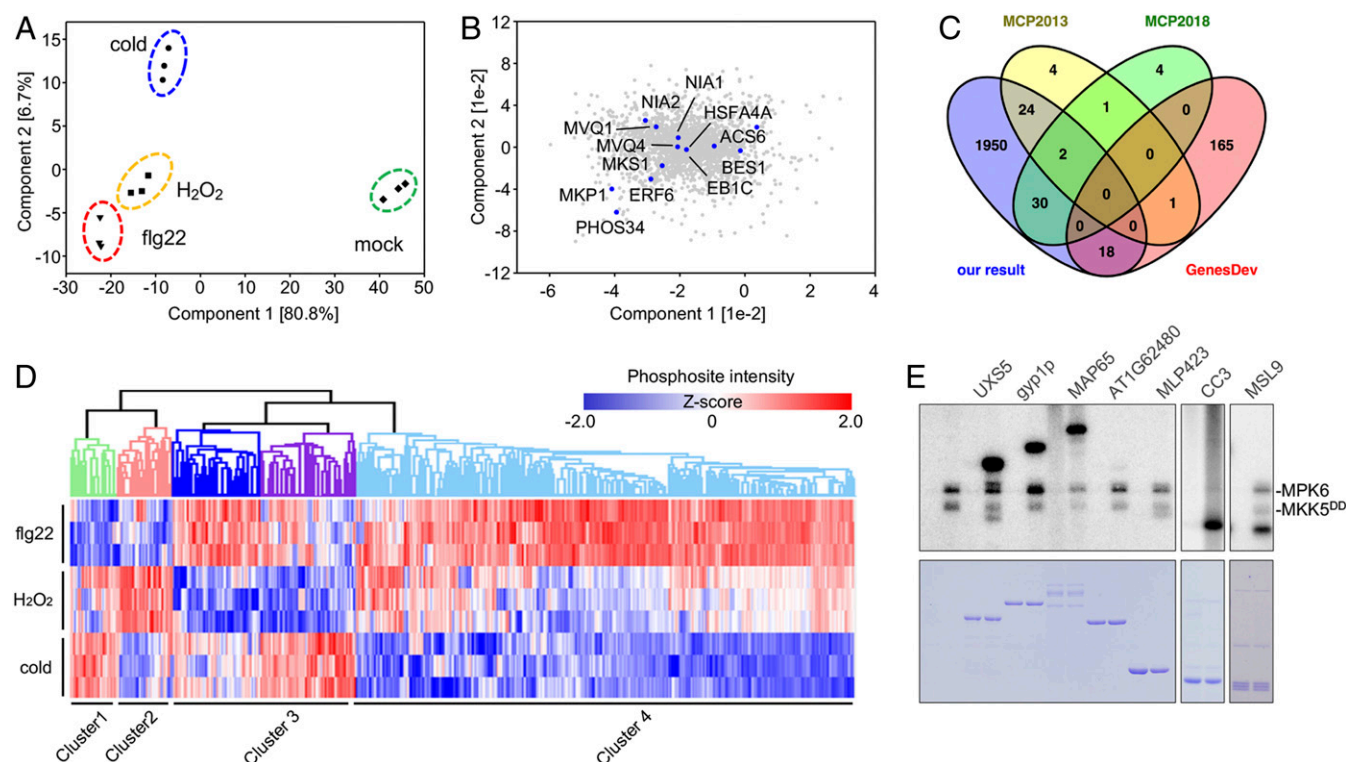


Fig. 2. Identification of putative MPK6 substrates using KALIP 2.0. (A) PCA of the identified O¹⁸-phosphorylation sites across four samples. The first component separates four samples based on the stress treatment (left) versus control (right), and the second component distinguishes cold stress (up) versus H₂O₂ and pathogen stress (down). (B) PCA of the distribution of direct MPK substrates identified by the KALIP 2.0 method. Previously reported MPK substrates were highlighted. (C) Venn diagram showing the overlap between the putative MPK6 substrates identified by our method in this study and by previous high-throughput studies. (D) Hierarchical clustering representing four distinct clusters of stress-induced MPK6 putative substrates (ANOVA, FDR < 0.05). Z-score normalized intensities for each O¹⁸-phosphorylation site are color-coded based on high (red) or low (blue) values. (E) Kinase assay showing that MPK6 phosphorylates several randomly selected putative substrates in vitro. (E, Top) Autoradiograph showing phosphorylation signals. (E, Bottom) Coomassie-stained gel showing the positions of substrate proteins.

Identification of Putative Targets and Phosphorylation Motifs of Protein Kinases in Response to Stresses.

Encouraged by the results from MPK6, we applied the KALIP 2.0 method to identify putative substrates of other protein kinases involved in abiotic and biotic stresses. These experiments included combinations between MPK6, SnRK2.4, SnRK2.6, CKL2, SOS2, calcium/calmodulin-regulated receptor-like kinase 2 (CRLK2), CPK11, oxidative signal-inducible1 (OXI1), and CIPK23 as kinases and osmotic stress, ABA, salt stress, flg22, oxidative stress, and potassium deficiency as stress treatments. The specific combinations tested are represented in Fig. 3A. In total, 5,075 unique proteins were identified as class I substrates of the 12 protein kinase/stimulus combinations tested (Fig. 3A and see also [Datasets S2–S13](#)). The number of class II and III substrates is also shown in Fig. 3A. No class III CIPK23 substrate was identified from the potassium starvation-treated samples, possibly due to the relatively weak CIPK23 kinase activity in vitro, and/or weak CIPK23 kinase activity in vivo after the plants were transferred to low potassium conditions for 12 h (Fig. 3A). The clustering of the class I substrates of these kinase/stimulus combinations is shown in Fig. 3B. These results suggest that different kinases may have similar targets upon activation by a specific stress condition (e.g., OXI1 and MPK6 substrates upon H₂O₂ treatment), suggesting a certain degree of redundancy in the phosphorylation of proteins mediating stress responses. Interestingly, a single kinase, MPK6, seems to phosphorylate the same substrates even upon activation by different stresses (Fig. 3B), although the phosphorylation levels of the targets under different stresses vary (Fig. 2D). This finding supports the notion that the differential expression of the

substrates is a major determinant of substrate specificity in MAPK cascades (42). To understand the biological function of the putative substrates of each of the protein kinases, GO analysis was performed (Fig. 4A). In keeping with our previous reasoning, MPK6 substrates upon activation by four different stresses have similar GO terms, while the substrates of other protein kinases show exclusive GO terms for their biological function (Fig. 4A).

This large-scale phosphopeptide identification allowed for the detection of phosphorylation motifs associated with specific kinases in stress conditions. Motif analysis using our data revealed that MPK6 mainly recognizes the pS/pTP motif and that SnRK2s and SnRK3s mainly recognize the LxRxxpS/pT and its variant LxxxxpS/pT or RxxpS/pT ([SI Appendix, Fig. S3](#)). Interestingly, SnRK2.6 also recognizes a GS motif. In a previous study, a GpSxxxxE motif was found to be enriched in ABF transcription factors (TFs), which are well-known SnRK2.6 substrates (31). However, in our results, only the glycine (G) at –1 position, but not the glutamic acid (E) at +5 position, is enriched in the putative SnRK2.6 substrates ([SI Appendix, Fig. S3](#)), which suggests that the E at +5 position may not be necessary for SnRK2.6 recognition. Finally, our analysis also shows that OXI1 mainly recognizes the pS/pTF phenylalanine motif ([SI Appendix, Fig. S3](#)) and that the pSF and pSxxL motifs are also enriched in several target sites of SOS2 ([SI Appendix, Fig. S3](#)).

Identification of SnRK2 and CKL2 Targets upon ABA and Osmotic Stress Treatments. ABA is a phytohormone important for plant responses to several abiotic stresses, including osmotic stress. In

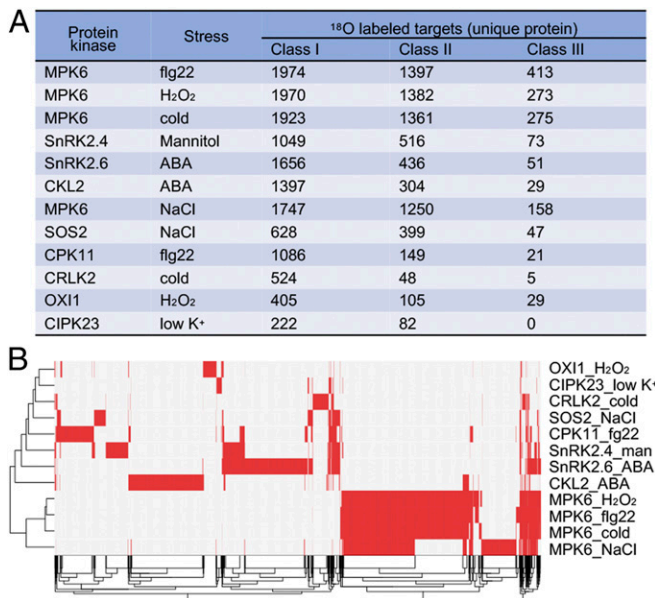


Fig. 3. Integrative analysis of the putative substrates identified in 12 kinase/treatment combinations. (A) Summary the class I, class II, and class III substrates from 12 protein kinase/treatment combinations. (B) Comparison of the putative substrates (unique proteins) identified from 12 protein kinase/treatment combinations. A large set of MPK6 substrates is shared among different treatments. In addition to their shared substrates, all of the tested kinases showed specific substrates.

total, we identified 1,049 and 1,656 unique proteins as putative direct targets of SnRK2.4 and SnRK2.6 in mannitol- or ABA-treated samples, respectively (Datasets S5 and S6). The list includes previously identified substrates such as ABA responsive element binding factor 1–4 (ABF1–4), enhanced late embryogenesis abundant level (EEL), ABA-responsive element binding protein 3 (AREB3), ABA-responsive kinase substrates (AKSs), VARICOSE, respiratory burst oxidase homolog D (RbohD), and SERRATE, and several proteins known to be involved in osmotic stress responses, such as cytosolic invertase 1 (CINV1) (43), soluble *N*-ethylmaleimide-sensitive factor adaptor protein 33 (SNAP33) (44), H⁺-ATPase 1 (OPEN STOMATA 2), and delta1-pyrroline-5-carboxylate dehydrogenase (P5CDH) (45). As expected, the major enriched GO terms of the putative SnRK2 targets identified in this work include response to osmotic stress and ABA signaling. Other enriched GO terms included cell growth and cell cycle, vesicle-mediated transport, microtubule-based movement, chromosome organization, reproductive developmental process, and embryonic and postembryonic development, revealing the importance of SnRK2s in the regulation of these processes in response to ABA and osmotic stress.

Our data support the notion that stress-activated SnRK2s target proteins that function in the regulation of gene expression. In addition to basic leucine zipper (bZIP) and basic helix–loop–helix TFs known to be putative substrates of ABA-activated SnRK2s (31, 32), we identified two C2H2 zinc finger family TFs and six homeodomain proteins as putative targets of SnRK2s (Dataset S14). Two of the homeodomain proteins, ABA insensitive growth 1 (ABIG1) and HOMEODOMAIN protein 6 (HB6), are known to regulate ABA response (46, 47). In addition to TFs, several proteins related to chromatin remodeling and modifications were identified as putative substrates of SnRK2s (Dataset S14), along with proteins functioning in messenger RNA (mRNA) decay and microRNA biogenesis (Dataset S14). The results suggest that, in addition to transcriptional regulation through the phosphorylation of TFs, posttranscriptional regulation is also important for

SnRK2-mediated regulation of gene expression in response to osmotic stress. SnRK2s also regulate osmolyte synthesis and sugar metabolism (12). Our phosphoproteomics data support this notion, since 44 phosphoproteins (1.8-fold enriched, $P = 0.015$) involved in different steps of carbohydrate biosynthetic processes were identified as putative substrates of SnRK2s (Datasets S5 and S6). The data suggest that SnRK2s regulate multiple enzymes to alter carbohydrate metabolism upon osmotic stress. The adaptation to osmotic stress also involves alterations in the composition of the cell wall (48). Our data reveal that SnRK2s phosphorylate the xyloglucan galactosyltransferase RSA3 (short root in salt medium 3) and several enzymes involved in beta-glucan metabolic processes (Dataset S14), suggesting that SnRK2s mediate metabolic changes in the cell wall in response to osmotic stress.

We also identified proteins functioning in vesicle trafficking among osmotic stress-activated SnRK2 targets, including four SNARE (soluble *N*-ethylmaleimide-sensitive fusion protein attachment protein receptors) proteins (49) and two SNARE-related proteins (Datasets S5, S6, and S14). These proteins are required for ABA-controlled gating of K⁺ and Cl[−] channels (50, 51) and control the trafficking of plasma membrane aquaporin and cellular osmotic homeostasis (52). The identification of these phosphoproteins in our study provides a biochemical link between the ABA-mediated activation of SnRK2s and the regulation of these processes in response to osmotic stress.

The identification of putative kinase substrates is particularly powerful in combination with genetic evidence about the function of the studied kinases or their substrates. Through the phenotypic analysis of a *snrk2.1/2/3/4/5/6/7/8/9/10* decuple mutant, we previously found that SnRK2s are important for the accumulation of the second messenger inositol 1,4,5-trisphosphate and the compatible osmolyte proline in response to osmotic stress (12, 53). In this study, we found that an important group of putative SnRK2 substrates are related to the regulation of phosphoinositide production, such as phosphoinositide 4-kinase β 1 (PI4K β 1), phosphatidylinositol-4-phosphate 5(PIP5)-kinases, and phospholipase C1 (PLC1) (Dataset S14), providing a biochemical explanation to the requirement of SnRK2s for stress-induced accumulation of phosphoinositides. The identification of P5CDH (Dataset S14) as a putative SnRK2 target helps to explain why osmotic stress-induced proline accumulation was reduced in the decuple mutant (12, 53).

Both SnRK2.6 and CKL2 function in the ABA signaling network (18). Among the CKL2 putative substrates, we identified four high-mobility group B proteins (HMGB1 to HMGB4) (Dataset S14), two of which, HMGB1 and HMGB2, are known to participate in ABA signaling and salt stress responses (54, 55). Moreover, we found that the putative CKL2 target proteins include proteins that function in RNA splicing, chromatin organization, and vesicle-mediated and intracellular transport (Fig. 4 A and B and Dataset S14). CKL2 phosphorylates a set of proteins involved in histone methylation and acetylation, such as the histone acetyltransferase general control nonderepressible 5 (GCN5), HISTONE DEACETYLASE 6 (HDA6), histone methyltransferase homolog of anti-oxidant 2 (ATX2), early flowering in short days (EFS), as well as histone binding proteins VERNALIZATION 5 (VRN5), nucleosome assembly protein 1 (NAP1)-related protein 2 (NRP2), and terminal flower2 (TFL2). GCN5 and HDA6 are known to function in the transcriptional regulation of cold- and drought-responsive genes (56, 57). Interestingly, several putative target proteins of CKL2 have important functions in vernalization and flowering, namely VRN5, TFL2, FIE, and EFS, revealing a potential novel function of CKL2 in flowering time regulation. Furthermore, the list of CKL2 putative targets includes 16 proteins with the GO term vesicle-mediated transport, including two exocyst subunit EXO70 family proteins, EXO70D2 and EXO70H8, four adaptins, Golgi vesicle-mediated transport proteins ATGRIP, HopM1 interactor 7

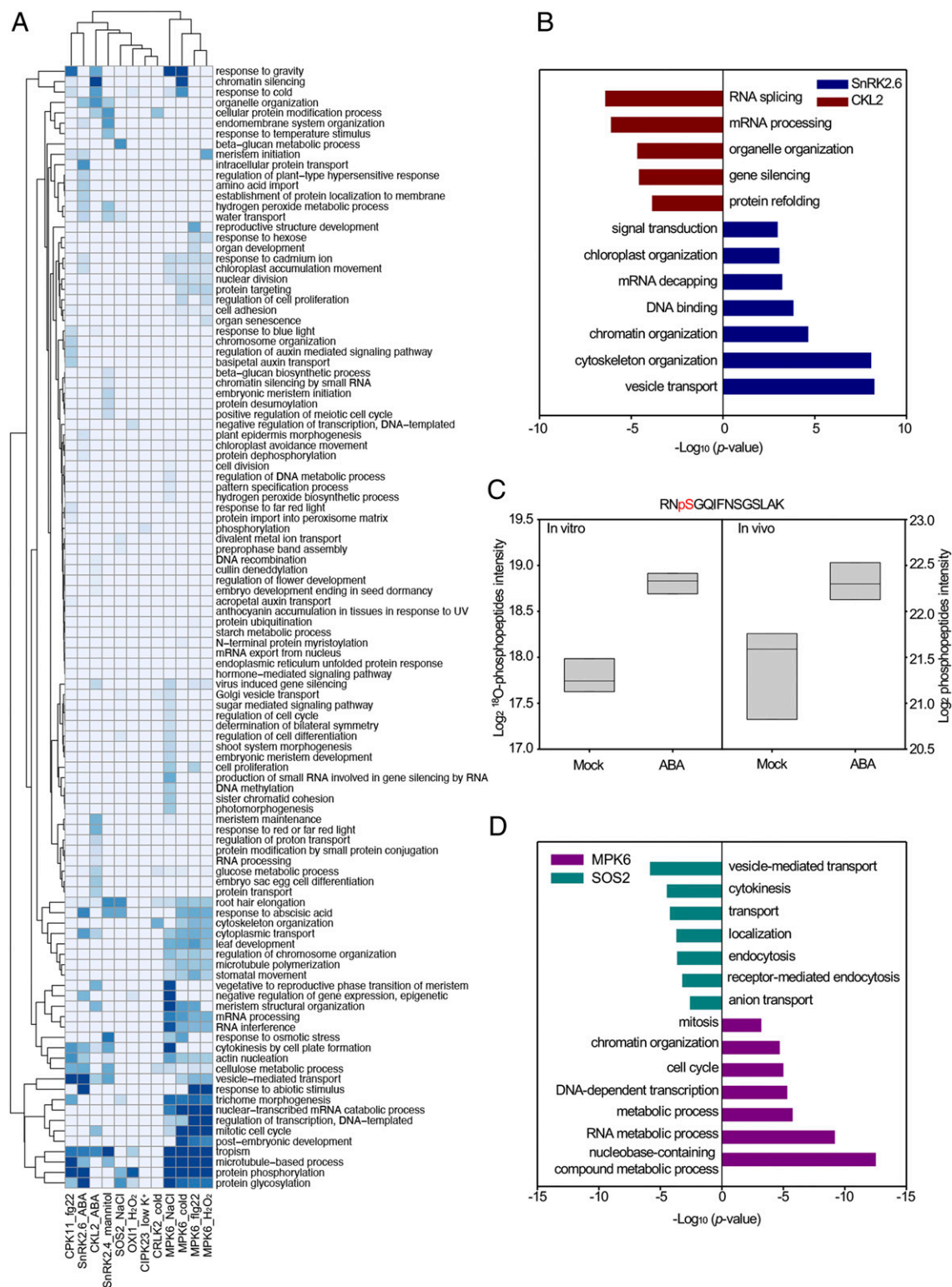


Fig. 4. Proteomic signature of the putative substrates (unique proteins) identified from 12 protein kinase/treatment combinations. (A) GO analysis of the putative substrates (unique proteins) identified from 12 protein kinase/treatment combinations. (B) Bar chart highlighting enriched categories of GO biological function in putative SnRK2.6 and CKL2 substrates identified from ABA-treated seedlings using Fisher's exact test (Benjamini–Hochberg FDR < 0.05). (C) CKL2 is a class III putative substrate of SnRK2.6. The phosphopeptide RNP5GQIFN5GSLAK was identified both in vitro and in vivo, and its level was significantly increased in ABA-treated samples in both the in vitro and in vivo comparisons (two-sample *t* test, FDR < 0.05). (D) Dark cyan and pink bars representing significant GO categories in putative SOS2 and MPK6 substrates identified from NaCl-treated seedlings (Benjamini–Hochberg FDR < 0.05).

(MIN7), and Golgin Candidate 6 (GC6). Another GO term enriched in the putative CKL2 targets is RNA splicing (Dataset S14). Our findings suggest a novel regulatory role of CKL2 in modulating flowering time as well as in specific cellular functions such as vesicle trafficking and RNA splicing.

Motif analysis of the putative CKL2 targets identified in our study suggests that CKL2 recognizes the acidic motif pS/TD/ED/ED/E (SI Appendix, Fig. S3). This acidic motif is one of the motifs in ABA-responsive phosphoproteins identified in our previous phosphoproteomics study (32). To further investigate the function of CKL2 in ABA-responsive phosphorylation as well as the relationship between SnRK2 and CKL2, we carried out a pairwise comparison of ABA up-regulated phosphoproteins in the wild type and *snrk2* decuple mutant (2). Of a total of 9,913 quantified phosphopeptides, ABA treatment increased the abundance of 948 phosphosites from 801 unique phosphoproteins in the wild type, and 247 phosphosites from 219 unique phosphoproteins were up-regulated in the *snrk2* decuple mutant. Only 14 phosphosites were up-regulated in both the wild type and *snrk2* decuple mutant. Among the 934 SnRK2-dependent ABA-up-regulated phosphosites, 172 contained the S/TD/ED/ED/E acidic motif. Additionally, 265 SnRK2-dependent ABA-up-regulated phosphosites contained the LxR/KxxS/T motif, which is possibly recognized by SnRK2s. Interestingly, CKL2 was identified as a class III substrate of SnRK2.6 upon ABA treatment, with the phosphopeptide RNP SGQIFNSGSLAK significantly up-regulated in both the in vivo and in vitro phosphoproteomics analyses (Fig. 4C). Taken together, these results suggest that SnRK2 and CKL2 may work in concert to regulate gene transcription, RNA splicing, vesicle transport, metabolism, and epigenetic states (Fig. 4B).

Role of SOS2 and MPK6 in Salt-Stress Responses. Although it has long been known that SOS2 is critical for salt tolerance (19) and that MPK6 is quickly activated upon salt stress (36, 58), few substrates of SOS2 and MPK6 in response to salt stress have been identified. In our experiments, 1,747 class I targets, 1,250 class II targets, and 158 class III targets of MPK6 were identified from NaCl-treated samples (Dataset S8). The GO terms specifically enriched among these putative MPK6 targets include mRNA processing, transcription, chromatin modification, cell growth, and system development (Fig. 4A and D). Interestingly, these MPK6 targets include a subset of proteins with known roles in salt stress responses, such as Na^+/H^+ EXCHANGER1/2 (NHX1/2), which are tonoplast-localized $\text{Na}^+/\text{K}^+/\text{H}^+$ exchangers important for Na^+/K^+ uptake into the tonoplast (59) (Dataset S14). Previous studies have shown that salt stress leads to the alternative splicing of more than 1,000 genes (60), suggesting the importance of RNA splicing in salt-stress responses. We found that 18 splicing factors are putative direct targets of MPK6 upon salt stress (Dataset S8), including AT1G60200, which is involved in plant response to salinity and ABA (61). Therefore, our results provide a link between the activation of salt signaling and specific stress responses, mediated by MPK6 phosphorylation of these substrates. In addition, a set of proteins involved in meristem initiation was also identified as putative targets of MPK6 (Dataset S14), supporting a role of MPK6 in regulating plant development under salt stress conditions.

The same samples used for the MPK6 study were also subjected to in vitro kinase assays using a constitutively activated form of SOS2, SOS2CA^{S228D} (62). From this analysis, we identified 628 class I, 399 class II, and 47 class III targets of SOS2 (Dataset S9). We found several GO terms enriched among these putative SOS2 targets, including intracellular transport, monosaccharide and polysaccharide biosynthetic process, ABA-mediated signaling pathway, sugar-mediated signaling pathway, cytoskeleton organization, and cell-wall biogenesis (Fig. 4A and D). Consistent with the critical role of SOS2 in the regulation of ion homeostasis, SOS2 phosphorylated several ion transporters (Datasets S8 and

S14), including cation exchanger 1 (CAX1), which is a known SOS2-interacting protein (63). This result suggests that SOS2 may activate the $\text{Ca}^{2+}/\text{H}^+$ antiporters through direct phosphorylation. Three chloride channels were also identified as putative direct substrates of SOS2, including chloride channel-C (CLC-C), which is critical for NaCl tolerance in *Arabidopsis* (64, 65) (Dataset S14). It is noteworthy that the putative substrates of SOS2 are not enriched in proteins involved in transcription and mRNA processing, cell growth, or system development. This is consistent with the limited role of SOS2 in regulating gene expression (19) and a lack of growth or developmental phenotypes of loss-of-function *sos2* mutant plants (66, 67).

Interestingly, proteins associated with specific stress-related processes were found as putative targets of both MPK6 and SOS2 in our analysis. Cortical microtubule organization is important for salt-stress tolerance (68, 69). We found that tubulins and several tubulin-associated proteins are putative targets of MPK6 and SOS2 upon salt stress (Dataset S14), including microtubule-associated protein 65-1 (MAP65-1), which is a known MPK6 substrate and controls microtubule organization in response to salt stress (70, 71). SOS2 may also regulate the organization of the actin cytoskeleton by phosphorylating several actin and actin-associated proteins (Dataset S14). Similarly, a set of cellulose synthase (CESA) and CESA-like proteins, required for cell wall synthesis, was identified as direct targets of MPK6 and SOS2 upon salt stress (Dataset S14). It has been suggested that phosphorylation is critical for the regulation of CESA activity (72). Moreover, we found that three CC proteins, which regulate microtubule organization and cellulose synthase localization under salt stress by promoting microtubule dynamics (73), are putative targets of MPK6. Our data indicate that MPK6 and SOS2 are probably key regulators of phosphorylation-mediated rearrangements in cytoskeleton and cell-wall organization upon salt stress. Moreover, the identification of specific phosphorylation sites provides valuable information for future studies to understand the phosphorylation-mediated regulation of multiple proteins associated with these processes.

Identification of Substrates of CPK11 in the Activation of Plant Immunity. To identify the downstream targets of calcium-dependent protein kinases (CPKs) upon activation of plant immune responses, the KALIP 2.0 method was applied to flg22-treated samples incubated with CPK11, a CPK involved in immune signaling (7). As a result, 2,217 phosphopeptides from 1,086 unique proteins was labeled by ^{18}O -ATP in the presence of recombinant CPK11 (Dataset S10). Interestingly, the list of CPK11 targets includes the NADPH oxidase RbohD, which is responsible for the generation of reactive oxygen species upon flg22 perception, and a known substrate of immune-activated CPK5 (74).

A set of TFs associated with plant immunity was identified as putative substrates of CPK11 (Dataset S14), including WRKY DNA-binding protein 33 (WRKY33), which has been reported as an MPK6 substrate (75). In addition to WRKY33, 21 TFs were identified as putative targets of CPK11 and MPK6 upon flg22 treatment, including WRKY3 and WRKY15 (Dataset S14). The overlap between CPK11 and MPK6 targeted TFs may help explain the reported synergistic effect between MAPK- and CDPK-dependent regulation of defense-related genes (7). Besides transcriptional regulators, CPK11 substrates included several cell surface seven-transmembrane (7TM) domain receptors (Dataset S14), known to be critical for the sensing of fungal contact (76). Among them, mildew resistance locus O 8 (MLO8) and MLO12 are known to confer resistance to powdery mildew in *Arabidopsis* (77). We also found that five myosin family motor proteins are putative targets of CPK11 (Dataset S14). The myosin family of molecular motors move cargo on actin filaments and are required for resistance to the penetration of fungal pathogens (78). Myosin and actin filamentation is also required for the

recruitment of PENETRATION (PEN) proteins at the fungal infection site, which contribute to disease resistance (79). Remarkably, we also found PEN1 and PEN3 (78) as putative substrates of CPK11. The identification of numerous proteins involved in the response to fungal pathogens as substrates of flg22-activated CPK11 may explain the observed requirement for CPK11 (together with CPK5/6) for the flg22-induced resistance to fungal pathogens (80), in keeping with the notion that CPKs act as signaling nodes upon calcium-mediated activation by both bacterial and fungal pathogens (81). Overall, our work reveals a potential central role of CPK11 in the activation of defense responses to fungal infection at the cell surface and provides a phosphorylation-mediated mechanism for the activation of these responses.

Application of KALIP 2.0 to Other Stress-Related Kinases. To take further advantage of the KALIP 2.0 method, we sought to identify putative substrates of additional kinases related to the plant response to environmental stresses. For this analysis, we included OXI1, a protein kinase A, G, and C family (AGC) protein kinase that participates in the plant response to oxidative stress and pathogen infection (82), CIPK23, which is activated in conditions of low-potassium (83), and CRLK2, a calcium/calmodulin-regulated receptor-like kinase, which regulates cold-responsive gene expression and freezing tolerance (84, 85). In this analysis, we found that 405 and 105 proteins were identified as class I and class II putative substrates of OXI1 activated by treatment with H_2O_2 , respectively (Dataset S11). Among these substrates, we found autoinhibited Ca^{2+} -ATPases, ISOFORM 8 (ACA8) and ACA10, which are plasma membrane localized Ca^{2+} -ATPases required for stimulus-induced calcium signaling (86). The function of ACA8 in calcium signaling is regulated by phosphorylation at its N-terminal region (87). In keeping with this notion, our data include an ^{18}O -labeled phosphopeptide (KSEHADSDDTFYIPSKN), present at the N-terminal regions of both ACA8 and ACA10. The presence of ACA8 and ACA10 as putative targets of OXI1 suggests a putative role of OXI1 in the regulation of calcium signaling in response to H_2O_2 and pathogen infection. This is consistent with the fact that both ACA8 and ACA10 interact with BONZAI 1 (BON1), a calcium-dependent, phospholipid binding protein that regulates plant immunity (88). Moreover, we found several other proteins related to calcium signaling among OXI1 substrates (Dataset S14), including calmodulins, calmodulin-binding proteins, CPKs, and other EF hand-containing proteins, further supporting the role of OXI1 in the regulation of calcium signaling. Consistent with the notion that OXI1 is involved in plant immunity, we also identified the *Arabidopsis* chitin receptor, chitin elicitor receptor kinase 1 (CERK1), as a putative substrate of OXI1.

Using CIPK23 and low-potassium-treated samples, we found 222 class I and 80 class II putative substrates (Dataset S12). Among these substrates, we identified three potassium transporters, including potassium uptake transporter 4 (KUP4), which is required for tip growth in *Arabidopsis* root hairs (89). Additionally, we identified a set of proteins that regulate auxin signaling and root development (Dataset S14), suggesting a potential role of CIPK23 and its substrates in regulating root architecture upon potassium starvation.

Using cold-stress treatment, we identified 514 class I, 48 class II, and 7 class III substrates of CRLK2. Among them, MKK2 and STABILIZED1 (STA1) are known to function in cold-stress responses. Upon cold stress, MKK2 is phosphorylated by the upstream kinase MEKK1 and then phosphorylates downstream MPK6 to promote the degradation of Inducer of C-REPEAT/DRE BINDING FACTOR (CBF) expression 1 (ICE1) (36, 85). Although the relationship between CRLKs and these regulators still needs to be validated, our results provide

important clues into the biochemical function of CRLKs in cold-stress responses.

Common Targets of Stress-Activated Protein Kinases. In this study, we noticed that many proteins could serve as direct targets of multiple protein kinases (Fig. 5A), including proteins functioning in tropism, cellulose metabolic process, cytoskeleton, transport, and cell organization (Fig. 5B). For example, VLN3, a Ca^{2+} -regulated villin protein involved in actin filament bundling (90, 91), was identified as a class II substrate of MPK6, SnRK2.4, SnRK2.6, SOS2, CPK11, and CRLK2 and a class I substrate of CKL2. To validate this result, we performed gel-based in vitro kinase assays and showed that VLN3 is indeed phosphorylated by MPK6, CKL2, CRLK2, SOS2, SnRK2s, and CPK11, but not by CIPK23 (Fig. 5C and D). The phosphorylation signals from CRLK2 and SOS2 were relatively weak, likely due to their low kinase activity in comparison with MPK6, CKL2, SnRK2, and CPK11. Interestingly, although all of our identified phosphosites of VLN3 are localized in a small region between the last actin-depolymerizing factor homology (ADF-H) domain and villin headpiece (VHP) domain, different kinases seem to phosphorylate different sites. For example, we found that MPK6 phosphorylates Ser696 and Ser809, while SnRK2.4 and SnRK2.6 phosphorylate Ser768 and Ser836, CPK11 phosphorylates Ser826, and SOS2 phosphorylates Ser836 (Fig. 5C). Phosphorylation at different sites may mediate different responses triggered by different stresses, suggesting a potential phosphorylation code for the regulation of these proteins. Although further functional validation is required, it is tempting to speculate that these common target proteins may constitute common hubs in plant signaling and responses triggered by different environmental stresses through phosphorylation mediated by various stress-responsive kinases.

Conclusions

Although protein kinases are critical for cellular signaling, the identification of kinase substrates is still challenging. The KALIP 2.0 method that we report here follows a simple and straightforward pipeline and takes advantage of the use of phosphopeptides as substrate pool to significantly reduce the complexity of kinase reactions and a two-step enrichment of phosphopeptides to increase the capability to detect low-abundance substrates. Our method provides unprecedented resolution and robustness in the identification of direct targets of protein kinases. Using this method, we identified more than 5,000 putative targets of 12 protein kinase/stress combinations. It is noteworthy that more than 14% (717 out of 5,076) of these putative targets were also phosphorylated in vivo, and their phosphorylation was enhanced under stress conditions. In vitro gel-based assays using randomly selected targets showed that they were indeed phosphorylated when recombinant proteins were used as substrates, validating the phosphoproteomics results. Additionally, this method allows for the identification of specific motifs phosphorylated by different kinases and provides the sites phosphorylated within these motifs. Although using peptides as substrate pool helps to reduce the complexity of the kinase reactions, it is possible that without the docking sequence and protein-protein-based recognition, peptide-based in vitro phosphorylation assay might miss some real substrates. The MS-based phosphoproteomics methods may also miss extreme low-abundance substrates and proteins unsuitable for MS detection. At the same time, certain kinases may unspecifically phosphorylate peptides containing similar motifs to their actual substrates (e.g., S/TP for MAPK and CDK), resulting in false positives. Nevertheless, our results showed that the closely related SnRK2.6 and SnRK2.4 differ in many of their putative targets, which suggests that certain kinases can keep their specificity even at the peptide level. Moreover, we classified the identified peptides based on their specific detection under stress conditions and the simultaneous identification of their

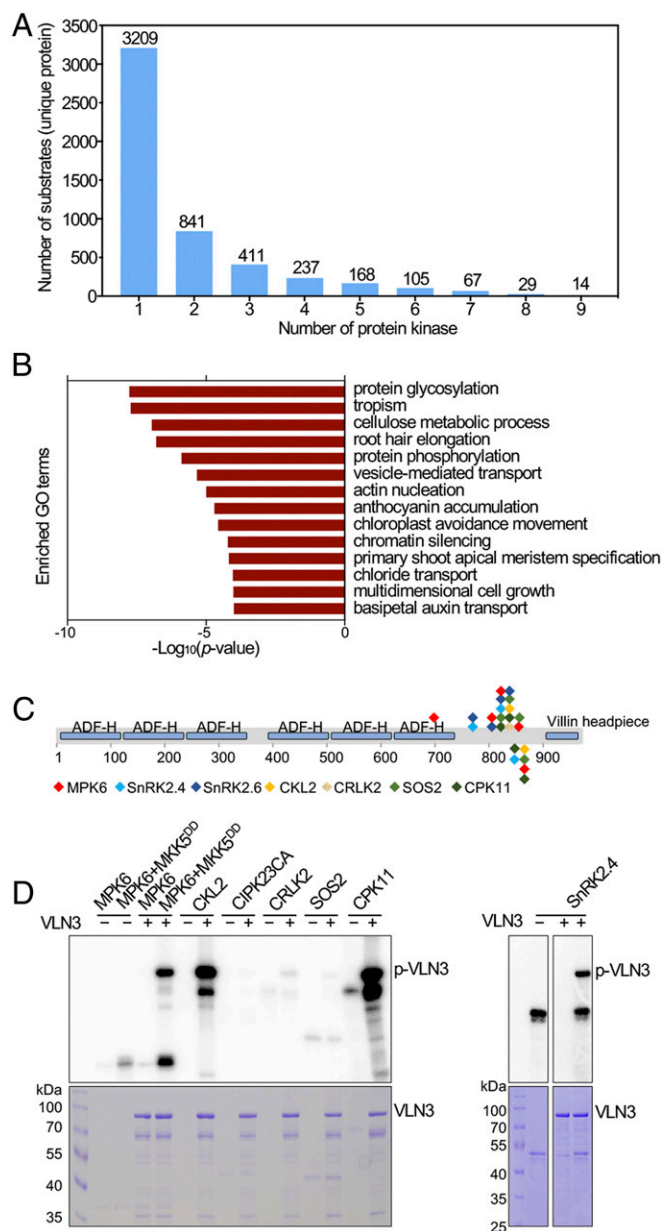


Fig. 5. Putative common targets of stress-activated protein kinases. (A) Several proteins are phosphorylated by multiple protein kinases. The x axis shows the number of protein kinases that phosphorylated the putative substrates, and the y axis shows the number of substrates (unique proteins). (B) Enriched GO terms of proteins that were phosphorylated by at least five protein kinases in our study. (C). Putative phosphosites identified in VLN3 in our study. The phosphosites corresponding to different protein kinases are indicated by different colors. (D) In vitro kinase assay validating that VLN3 could be phosphorylated by multiple protein kinases. Autoradiograph (Top) and Coomassie staining (Bottom) show phosphorylation and loading of purified VLN3 protein and different protein kinases.

phosphorylation in vivo. Such classification helps to minimize false-positive hits and nonspecific substrates and allows for the selection of appropriate candidate substrates to perform further biochemical validation or functional analysis.

Our work shows that KALIP 2.0 is a powerful tool for identifying substrates of protein kinases in response to environmental stimuli, yielding insights into the roles of different kinases and their putative targets in specific stress response pathways. The application of KALIP 2.0 acquires a new dimension when

combined with previous findings from genetic analysis. In such cases, our results not only contribute to the reinforcement of previous findings, but, more importantly, also provide biochemical links between the perception of environmental stresses and the subsequent activation of cellular responses. The identification of specific phosphorylation sites in the interaction between the kinases and known regulators of environmental stress responses provides valuable data to understand the mechanisms of activation for these regulators.

Even though we focused on protein kinases activated by environmental stresses in this study, KALIP 2.0 may be applied to other protein kinases involved in virtually any plant process. We believe that this method is applicable to phosphorylation studies in various biological systems, including nonplant systems, and can be integrated with other resources, such as genetic mutants, for system-wide studies of kinase–substrate networks.

Materials and Methods

Plant Materials. Seeds of *A. thaliana* were surface-sterilized for 10 min in 20% bleach and then rinsed four times in sterile deionized water. After germination and growth on half-strength Murashige and Skoog plates for 7 d, the seedlings were transferred to flasks containing 40 mL of half-strength Murashige and Skoog medium in continuous light on a rotary shaker set at 100 rpm. After 3 d, the medium in the flasks was exchanged for fresh medium for control or fresh medium containing 50 μ M ABA, 100 mM NaCl, 500 mM mannitol, 2 mM H₂O₂, or 10 μ M flg22 for treatment for 30 min. For cold treatment, precooled medium was used, and the seedlings were treated at 4 °C for 30 min before harvest. For low potassium treatment, the seedlings were transferred to medium containing 10 μ M K⁺ for 24 h.

Protein Extraction and Digestion. Plant sample preparation was performed as previously described (92). Briefly, the tissues were ground with liquid nitrogen in a mortar, and the ground tissues were lysed in 6 M guanidine hydrochloride containing 100 mM Tris-HCl (pH = 8.5) with ethylenediaminetetraacetic acid-free protease inhibitor mixture (Roche) and phosphatase inhibitor mixture (Sigma-Aldrich). Proteins were reduced and alkylated with 10 mM Tris-(2-carboxyethyl)phosphine and 40 mM chloroacetamide at 95 °C for 5 min. Alkylated proteins were subject to methanol-chloroform precipitation, and precipitated protein pellets were solubilized in 1% sodium deoxycholate (SDC) and 1% sodium lauryl sarcosinate (SLS). Protein concentration was quantified using a bicinchoninic acid assay (Thermo Fisher Scientific). Protein extracts were diluted to 0.2% SDC and SLS and digested with Lys-C (Wako) in a 1:100 (wt/wt) enzyme-to-protein ratio for 3 h at 37 °C and further diluted to a 1 M urea concentration. Trypsin (Promega) was added to a final 1:100 (wt/wt) enzyme-to-protein ratio and kept overnight. Digests were acidified with 10% trifluoroacetic acid (TFA) to a pH ~2 and desalted using a 100 mg of Sep-pak C18 column (Waters).

Stable Isotope-Labeled In Vitro Kinase Reaction. The tryptic phosphopeptides (400 μ g) from mock-treated and stress-treated seedlings were enriched by polyMAC (93). The enriched phosphopeptides were treated with thermo-sensitive alkaline phosphatase (Roche) in a 1:100 (wt/wt) enzyme-to-peptides ratio at 37 °C overnight for dephosphorylation, and the dephosphorylated peptides were desalted using SDB-XC StageTips. The desalted peptides were resuspended in kinase reaction buffer (50 mM Tris-HCl, 10 mM MgCl₂, 1 mM dithiothreitol, and 1 mM γ -[¹⁸O₄]ATP, pH 7.5). The recombinant kinase (1 μ g) was incubated with the desalted peptides at 30 °C overnight. The kinase reaction was quenched by acidifying with 10% TFA to a final concentration of 1%, and the peptides were desalted by SDB-XC StageTip. The heavy ¹⁸O-phosphopeptides were further digested by trypsin at 37 °C for 6 h and enriched by second polyMAC, and the eluates were dried in a SpeedVac for LC-MS/MS analysis.

In Vivo Phosphoproteomic Enrichment. Phosphopeptide enrichment was performed according to the reported polyMAC protocol with some modifications. Briefly, the digested peptides were resuspended with 20 μ L of ultrapure water, 200 μ L of loading buffer (50 mM glycolic acid in 0.5% TFA and 95% acetonitrile [ACN]) was added, and the sample was vortexed. Next, 50 μ L of the PolyMAC slurry were added to the sample and incubated for 15 min. The solution and polyMAC slurry were transferred into a 200- μ L tip with a frit and spun down for 2 min at 200 \times g. The slurry beads were washed with 200 μ L of loading buffer twice. The beads were washed with 200 μ L of washing buffer (80% ACN in double-distilled H₂O) for 5 min and

spun down for 2 min at 200 × g. Finally, the phosphopeptides were eluted twice with 50 µL of elution buffer (400 mM NH₄OH in 50% ACN) by spinning down for 2 min at 200 × g. The eluates were combined and completely dried in a SpeedVac. Basic pH reverse-phase fractionation was performed with some modifications as previously described (94).

LC-MS/MS Analysis. The phosphopeptides were dissolved in 5 µL of 0.3% formic acid (FA) with 3% ACN and injected into an Easy-nLC 1000 (Thermo Fisher Scientific). Peptides were separated on a 45-cm in-house packed column (360 µm outside diameter × 75 µm inside diameter) containing C18 resin (2.2 µm, 100 Å; Michrom Bioresources) with a 30-cm column heater (Analytical Sales and Services) and the temperature was set at 50 °C. The mobile phase buffer consisted of 0.1% FA in ultrapure water (buffer A) with an eluting buffer of 0.1% FA in 80% ACN (buffer B) run over a linear 60-min gradient of 6 to 30% buffer B at flow rate of 250 nL/min. The Easy-nLC 1000 was coupled online with a Velos LTQ-Orbitrap mass spectrometer (Thermo Fisher Scientific). The mass spectrometer was operated in the data-dependent mode to perform a full-scan MS (from *m/z* 350 to 1,500 with the resolution of 30,000 at *m/z* 400). The 10 most intense ions were subjected to collision-induced dissociation fragmentation (normalized collision energy 30%, AGC 3e4, maximum injection time 100 ms).

Data Processing. The raw files were searched directly against the *A. thaliana* (TAIR10) database with no redundant entries using MaxQuant software (version 1.5.5.1) with the Andromeda search engine. Initial precursor mass tolerance was set at 20 parts per million (ppm), the final tolerance was set at 6 ppm, and ion trap mass spectrometry MS/MS tolerance was set at 0.6 Da. Search criteria included a static carbamidomethylation of cysteines (+57.0214 Da) and variable modifications of 1) oxidation (+15.9949 Da) on methionine residues, 2) acetylation (+42.011 Da) at N terminus of protein, and 3) phosphorylation (+79.996 Da) on serine, threonine, or tyrosine residues were searched. For identification of ¹⁸O-phosphopeptides, heavy phosphorylation (+85.979 Da) was added as a variable modification, and the match between run function was enabled. Search was performed with trypsin/P digestion and allowed a maximum of two missed cleavages on the peptides analyzed from the sequence database. The FDRs of proteins, peptides, and phosphosites were set at 0.01. The minimum peptide length was six amino acids, and a minimum Andromeda score was set at 40 for modified peptides. A site localization probability of 0.75 was used as the cutoff for localization of phosphosites. All of the peptide spectral matches and MS/MS spectra were visualized using MaxQuant viewer. All of the localized and

up-regulated ¹⁸O-phosphosites under ABA stimulation were submitted to Motif-X and pLogo software to determine kinase phosphorylation motifs with TAIR10 database as background. The significance was set at 0.000001, the width was set at 13, and the number of occurrences was set at 20. PANTHER version 11 (95) was utilized to identify overrepresented GO with *P* value less than 0.05 and TAIR10 database was set as the background.

Quantitative Analysis. All data were analyzed by using the Perseus software (version 1.6.0.2). For quantification of *in vitro* kinase screening, the intensities of heavy ¹⁸O-phosphopeptides were extracted through MaxQuant, and the missing values of intensities were replaced by a constant value for statistical analysis. The significantly enriched ¹⁸O-phosphopeptides were identified by the *P* value is significant from a two-sample *t* test with a permutation-based FDR cutoff 0.01 with 50 was set at 0.35. For *in vivo* phosphoproteomic analysis, the significantly enriched phosphopeptides were identified by performing a two-sample *t* test with a permutation-based FDR cutoff 0.05 with 50 was set at 0.2. Normalization was carried out by subtracting the medium of log2-transformed phosphopeptide intensities.

Recombinant Protein Expression and In Vitro Kinase Assay. The coding regions of AT3G46440, AT1G24020, AT1G62480, AT4G13730, CC3, MAP65-1, CPK11, and OXI1 were amplified and inserted in frame into the plasmid pGEX-4T-1 or pMal-C2x and introduced into *E. coli* BL21 cells using the primers listed in *SI Appendix, Table S1*. Recombinant HIS-tagged MPK6, HIS-tagged MKK5^{DD} (85), MBP-tagged SnRK2.6, GST-tagged SnRK2.4, MBP-tagged CKL2, GST-tagged SOS2CA^{S228D} (62), MBP-tagged CPK11, GST-tagged OXI1, GST-tagged CIPK23, GST-tagged VLN3, UX55, MSL9, CC3, MLP423, gyp1p, and AT1G62480 were generated following standard protocols. For *in vitro* kinase assays, 0.2 µg protein kinase was incubated with 2 µg recombinant substrate proteins in 25 µL of reaction buffer (25 mM Tris-Cl, 10 mM MgCl₂, 1 mM MnCl₂ pH 7.5, and 0.1% β-mercaptoethanol) in the presence of 1 µM cold ATP, 5 µCi [³²P]ATP. After incubation at 25 °C for 30 min, the reaction was stopped by adding sodium dodecyl sulfate sample buffer and then subjected to sodium dodecyl sulfate polyacrylamide gel electrophoresis. Radioactivity was detected with a Personal Molecular Imager (Bio-Rad).

ACKNOWLEDGMENTS. This work was supported by the Chinese Academy of Sciences (J.-K.Z. and P.W.), including its Strategic Priority Research Program (Grant XDPB0404), and NIH Grant R01GM111788 (to W.A.T.). We thank Dr. Yan Guo, from the Chinese Agriculture University, for helpful discussions.

- Arabidopsis Genome Initiative, Analysis of the genome sequence of the flowering plant *Arabidopsis thaliana*. *Nature* **408**, 796–815 (2000).
- P. Wang *et al.*, Reciprocal regulation of the TOR kinase and ABA receptor balances plant growth and stress response. *Mol. Cell* **69**, 100–112.e6 (2018).
- S. Zhang, D. F. Klessig, MAPK cascades in plant defense signaling. *Trends Plant Sci.* **6**, 520–527 (2001).
- X. Meng, S. Zhang, MAPK cascades in plant disease resistance signaling. *Annu. Rev. Phytopathol.* **51**, 245–266 (2013).
- G. Tena, M. Boudsocq, J. Sheen, Protein kinase signaling networks in plant innate immunity. *Curr. Opin. Plant Biol.* **14**, 519–529 (2011).
- G. Tena, T. Asai, W. L. Chiu, J. Sheen, Plant mitogen-activated protein kinase signaling cascades. *Curr. Opin. Plant Biol.* **4**, 392–400 (2001).
- M. Boudsocq *et al.*, Differential innate immune signalling via Ca²⁺ sensor protein kinases. *Nature* **464**, 418–422 (2010).
- J. K. Zhu, Abiotic stress signaling and responses in plants. *Cell* **167**, 313–324 (2016).
- S. R. Cutler, P. L. Rodriguez, R. R. Finkelstein, S. R. Abrams, Absciscic acid: Emergence of a core signaling network. *Annu. Rev. Plant Biol.* **61**, 651–679 (2009).
- H. Fujii, J. K. Zhu, Arabidopsis mutant deficient in 3 abscisic acid-activated protein kinases reveals critical roles in growth, reproduction, and stress. *Proc. Natl. Acad. Sci. U.S.A.* **106**, 8380–8385 (2009).
- K. Nakashima *et al.*, Three Arabidopsis SnRK2 protein kinases, SRK2D/SnRK2.2, SRK2E/SnRK2.6/OST1 and SRK2I/SnRK2.3, involved in ABA signaling are essential for the control of seed development and dormancy. *Plant Cell Physiol.* **50**, 1345–1363 (2009).
- H. Fujii, P. E. Verslues, J. K. Zhu, Arabidopsis decuple mutant reveals the importance of SnRK2 kinases in osmotic stress responses *in vivo*. *Proc. Natl. Acad. Sci. U.S.A.* **108**, 1717–1722 (2011).
- M. Boudsocq, H. Barbier-Brygoo, C. Laurière, Identification of nine sucrose non-fermenting 1-related protein kinases 2 activated by hyperosmotic and saline stresses in *Arabidopsis thaliana*. *J. Biol. Chem.* **279**, 41758–41766 (2004).
- B. Brandt *et al.*, Calcium specificity signaling mechanisms in abscisic acid signal transduction in *Arabidopsis* guard cells. *eLife* **4**, e03599 (2015).
- D. Geiger *et al.*, Guard cell anion channel SLAC1 is regulated by CDPK protein kinases with distinct Ca²⁺ affinities. *Proc. Natl. Acad. Sci. U.S.A.* **107**, 8023–8028 (2010).
- T. Maierhofer *et al.*, Site- and kinase-specific phosphorylation-mediated activation of SLAC1, a guard cell anion channel stimulated by abscisic acid. *Sci. Signal.* **7**, ra86 (2014).
- M. M. Drerup *et al.*, The Calcineurin B-like calcium sensors CBL1 and CBL9 together with their interacting protein kinase CIPK26 regulate the Arabidopsis NADPH oxidase RBOHF. *Mol. Plant* **6**, 559–569 (2013).
- S. Zhao *et al.*, CASEIN KINASE1-LIKE PROTEIN2 regulates actin filament stability and stomatal closure via phosphorylation of actin depolymerizing factor. *Plant Cell* **28**, 1422–1439 (2016).
- J. K. Zhu, Salt and drought stress signal transduction in plants. *Annu. Rev. Plant Biol.* **53**, 247–273 (2002).
- R. Quan *et al.*, SCAPB/CBL10, a putative calcium sensor, interacts with the protein kinase SOS2 to protect Arabidopsis shoots from salt stress. *Plant Cell* **19**, 1415–1431 (2007).
- F. J. Quintero *et al.*, Activation of the plasma membrane Na/H antiporter Salt-Overly-Sensitive 1 (SOS1) by phosphorylation of an auto-inhibitory C-terminal domain. *Proc. Natl. Acad. Sci. U.S.A.* **108**, 2611–2616 (2011).
- J. Mok, H. Im, M. Snyder, Global identification of protein kinase substrates by protein microarray analysis. *Nat. Protoc.* **4**, 1820–1827 (2009).
- J. Ptacek *et al.*, Global analysis of protein phosphorylation in yeast. *Nature* **438**, 679–684 (2005).
- S. C. Popescu *et al.*, MAPK target networks in Arabidopsis thaliana revealed using functional protein microarrays. *Genes Dev.* **23**, 80–92 (2009).
- B. T. Houseman, J. H. Huh, S. J. Kron, M. Mrksich, Peptide chips for the quantitative evaluation of protein kinase activity. *Nat. Biotechnol.* **20**, 270–274 (2002).
- J. E. Huttel *et al.*, A rapid method for determining protein kinase phosphorylation specificity. *Nat. Methods* **1**, 27–29 (2004).
- J. A. Ubersax *et al.*, Targets of the cyclin-dependent kinase Cdk1. *Nature* **425**, 859–864 (2003).
- M. Loog, D. O. Morgan, Cyclin specificity in the phosphorylation of cyclin-dependent kinase substrates. *Nature* **434**, 104–108 (2005).
- N. Dephoure, R. W. Howson, J. D. Blethrow, K. M. Shokat, E. K. O'Shea, Combining chemical genetics and proteomics to identify protein kinase substrates. *Proc. Natl. Acad. Sci. U.S.A.* **102**, 17940–17945 (2005).
- Y. Yu *et al.*, Phosphoproteomic analysis identifies Grb10 as an mTORC1 substrate that negatively regulates insulin signaling. *Science* **332**, 1322–1326 (2011).
- T. Umezawa *et al.*, Genetics and phosphoproteomics reveal a protein phosphorylation network in the abscisic acid signaling pathway in *Arabidopsis thaliana*. *Sci. Signal.* **6**, rs8 (2013).

32. P. Wang *et al.*, Quantitative phosphoproteomics identifies SnRK2 protein kinase substrates and reveals the effectors of abscisic acid action. *Proc. Natl. Acad. Sci. U.S.A.* **110**, 11205–11210 (2013).
33. L. Xue *et al.*, Sensitive kinase assay linked with phosphoproteomics for identifying direct kinase substrates. *Proc. Natl. Acad. Sci. U.S.A.* **109**, 5615–5620 (2012).
34. L. Xue, P. Wang, P. Cao, J. K. Zhu, W. A. Tao, Identification of extracellular signal-regulated kinase 1 (ERK1) direct substrates using stable isotope labeled kinase assay-linked phosphoproteomics. *Mol. Cell. Proteomics* **13**, 3199–3210 (2014).
35. T. Asai *et al.*, MAP kinase signalling cascade in Arabidopsis innate immunity. *Nature* **415**, 977–983 (2002).
36. M. Teige *et al.*, The MKK2 pathway mediates cold and salt stress signaling in Arabidopsis. *Mol. Cell* **15**, 141–152 (2004).
37. Y. Kovtun, W. L. Chiu, G. Tena, J. Sheen, Functional analysis of oxidative stress-activated mitogen-activated protein kinase cascade in plants. *Proc. Natl. Acad. Sci. U.S.A.* **97**, 2940–2945 (2000).
38. K. Ichimura, T. Mizoguchi, R. Yoshida, T. Yuasa, K. Shinozaki, Various abiotic stresses rapidly activate Arabidopsis MAP kinases ATPMK4 and ATPMK6. *Plant J.* **24**, 655–665 (2000).
39. W. Hoehenwarter *et al.*, Identification of novel in vivo MAP kinase substrates in Arabidopsis thaliana through use of tandem metal oxide affinity chromatography. *Mol. Cell. Proteomics* **12**, 369–380 (2013).
40. N. Rayapuram *et al.*, Quantitative phosphoproteomic analysis reveals shared and specific targets of Arabidopsis Mitogen-Activated Protein Kinases (MAPKs) MPK3, MPK4, and MPK6. *Mol. Cell. Proteomics* **17**, 61–80 (2018).
41. T. Feilner *et al.*, High throughput identification of potential Arabidopsis mitogen-activated protein kinases substrates. *Mol. Cell. Proteomics* **4**, 1558–1568 (2005).
42. J. Xu, S. Zhang, Mitogen-activated protein kinase cascades in signaling plant growth and development. *Trends Plant Sci.* **20**, 56–64 (2015).
43. X. Qi *et al.*, AtCYT-INV1, a neutral invertase, is involved in osmotic stress-induced inhibition on lateral root growth in Arabidopsis. *Plant Mol. Biol.* **64**, 575–587 (2007).
44. Z. U. Nisa *et al.*, GsSNAP33, a novel Glycine soja SNAP25-type protein gene: Improvement of plant salt and drought tolerances in transgenic Arabidopsis thaliana. *Plant Physiol. Biochem.* **119**, 9–20 (2017).
45. O. Borsani, J. Zhu, P. E. Verslues, R. Sunkar, J. K. Zhu, Endogenous siRNAs derived from a pair of natural cis-antisense transcripts regulate salt tolerance in Arabidopsis. *Cell* **123**, 1279–1291 (2005).
46. T. Liu, A. D. Longhurst, F. Talavera-Rauh, S. A. Hokin, M. K. Barton, The Arabidopsis transcription factor ABIG1 relays ABA signaled growth inhibition and drought induced senescence. *eLife* **5**, e13768 (2016).
47. A. Himmelbach, T. Hoffmann, M. Leube, B. Höhener, E. Grill, Homeodomain protein ATHB6 is a target of the protein phosphatase ABI1 and regulates hormone responses in Arabidopsis. *EMBO J.* **21**, 3029–3038 (2002).
48. N. M. Iraki, R. A. Bressan, P. M. Hasegawa, N. C. Carpita, Alteration of the physical and chemical structure of the primary cell wall of growth-limited plant cells adapted to osmotic stress. *Plant Physiol.* **91**, 39–47 (1989).
49. R. Pratelli, J. U. Sutter, M. R. Blatt, A new catch in the SNARE. *Trends Plant Sci.* **9**, 187–195 (2004).
50. J. U. Sutter *et al.*, Absciscic acid triggers the endocytosis of the arabidopsis KAT1 K⁺ channel and its recycling to the plasma membrane. *Curr. Biol.* **17**, 1396–1402 (2007).
51. B. Leyman, D. Geelen, F. J. Quintero, M. R. Blatt, A tobacco syntaxin with a role in hormonal control of guard cell ion channels. *Science* **283**, 537–540 (1999).
52. A. Besserer *et al.*, Selective regulation of maize plasma membrane aquaporin trafficking and activity by the SNARE SYP121. *Plant Cell* **24**, 3463–3481 (2012).
53. Y. S. Rizzi *et al.*, P5CDH affects the pathways contributing to Pro synthesis after ProDH activation by biotic and abiotic stress conditions. *Front. Plant Sci.* **6**, 572 (2015).
54. D. L. Lildballe *et al.*, The expression level of the chromatin-associated HMGB1 protein influences growth, stress tolerance, and transcriptome in Arabidopsis. *J. Mol. Biol.* **384**, 9–21 (2008).
55. K. J. Kwak, J. Y. Kim, Y. O. Kim, H. Kang, Characterization of transgenic Arabidopsis plants overexpressing high mobility group B proteins under high salinity, drought or cold stress. *Plant Cell Physiol.* **48**, 221–231 (2007).
56. J. M. Kim *et al.*, Acetate-mediated novel survival strategy against drought in plants. *Nat. Plants* **3**, 17097 (2017).
57. E. J. Stockinger, Y. Mao, M. K. Regier, S. J. Triezenberg, M. F. Thomashow, Transcriptional adaptor and histone acetyltransferase proteins in Arabidopsis and their interactions with CBF1, a transcriptional activator involved in cold-regulated gene expression. *Nucleic Acids Res.* **29**, 1524–1533 (2001).
58. T. Munnik *et al.*, Distinct osmo-sensing protein kinase pathways are involved in signalling moderate and severe hyper-osmotic stress. *Plant J.* **20**, 381–388 (1999).
59. V. Barragán *et al.*, Ion exchangers NHX1 and NHX2 mediate active potassium uptake into vacuoles to regulate cell turgor and stomatal function in Arabidopsis. *Plant Cell* **24**, 1127–1142 (2012).
60. F. Ding *et al.*, Genome-wide analysis of alternative splicing of pre-mRNA under salt stress in Arabidopsis. *BMC Genomics* **15**, 431 (2014).
61. C. Cheng, Z. Wang, B. Yuan, X. Li, RBM25 mediates abiotic responses in plants. *Front. Plant Sci.* **8**, 292 (2017).
62. H. Fujii, J. K. Zhu, An autophosphorylation site of the protein kinase SOS2 is important for salt tolerance in Arabidopsis. *Mol. Plant* **2**, 183–190 (2009).
63. N.-H. Cheng, J. K. Pittman, J. K. Zhu, K. D. Herschi, The protein kinase SOS2 activates the Arabidopsis H⁽⁺⁾/Ca⁽²⁺⁾ antiporter CAX1 to integrate calcium transport and salt tolerance. *J. Biol. Chem.* **279**, 2922–2926 (2004).
64. M. Jossier *et al.*, The Arabidopsis vacuolar anion transporter, AtCLCg, is involved in the regulation of stomatal movements and contributes to salt tolerance. *Plant J.* **64**, 563–576 (2010).
65. R. Hu *et al.*, Overexpression of PP2A-C5 that encodes the catalytic subunit 5 of protein phosphatase 2A in Arabidopsis confers better root and shoot development under salt conditions. *Plant Cell Environ.* **40**, 150–164 (2017).
66. J. K. Zhu, J. Liu, L. Xiong, Genetic analysis of salt tolerance in arabidopsis. Evidence for a critical role of potassium nutrition. *Plant Cell* **10**, 1181–1191 (1998).
67. U. Halfter, M. Ishitani, J. K. Zhu, The Arabidopsis SOS2 protein kinase physically interacts with and is activated by the calcium-binding protein SOS3. *Proc. Natl. Acad. Sci. U.S.A.* **97**, 3735–3740 (2000).
68. T. Shoji *et al.*, Salt stress affects cortical microtubule organization and helical growth in Arabidopsis. *Plant Cell Physiol.* **47**, 1158–1168 (2006).
69. C. Wang, J. Li, M. Yuan, Salt tolerance requires cortical microtubule reorganization in Arabidopsis. *Plant Cell Physiol.* **48**, 1534–1547 (2007).
70. Q. Zhang *et al.*, Phosphatidic acid regulates microtubule organization by interacting with MAP65-1 in response to salt stress in Arabidopsis. *Plant Cell* **24**, 4555–4576 (2012).
71. M. Sasabe *et al.*, Phosphorylation of NtMAP65-1 by a MAP kinase down-regulates its activity of microtubule bundling and stimulates progression of cytokinesis of tobacco cells. *Genes Dev.* **20**, 1004–1014 (2006).
72. D. M. Jones *et al.*, The emerging role of protein phosphorylation as a critical regulatory mechanism controlling cellulose biosynthesis. *Front. Plant Sci.* **7**, 684 (2016).
73. A. Endler *et al.*, A mechanism for sustained cellulose synthesis during salt stress. *Cell* **162**, 1353–1364 (2015).
74. U. Dubiella *et al.*, Calcium-dependent protein kinase/NADPH oxidase activation circuit is required for rapid defense signal propagation. *Proc. Natl. Acad. Sci. U.S.A.* **110**, 8744–8749 (2013).
75. G. Mao *et al.*, Phosphorylation of a WRKY transcription factor by two pathogen-responsive MAPKs drives phytoalexin biosynthesis in Arabidopsis. *Plant Cell* **23**, 1639–1653 (2011).
76. C. A. Kumamoto, Molecular mechanisms of mechanosensing and their roles in fungal contact sensing. *Nat. Rev. Microbiol.* **6**, 667–673 (2008).
77. C. Consonni *et al.*, Conserved requirement for a plant host cell protein in powdery mildew pathogenesis. *Nat. Genet.* **38**, 716–720 (2006).
78. L. Yang *et al.*, Myosins XI modulate host cellular responses and penetration resistance to fungal pathogens. *Proc. Natl. Acad. Sci. U.S.A.* **111**, 13996–14001 (2014).
79. S. A. -H. Mackerness, C. F. John, B. Jordan, B. Thomas, Early signaling components in ultraviolet-B responses: Distinct roles for different reactive oxygen species and nitric oxide. *FEBS Lett.* **489**, 237–242 (2001).
80. M. Gravino, D. V. Savatin, A. Macone, G. De Lorenzo, Ethylene production in Botrytis cinerea- and oligogalacturonide-induced immunity requires calcium-dependent protein kinases. *Plant J.* **84**, 1073–1086 (2015).
81. J. Bigeard, J. Colcombet, H. Hirt, Signaling mechanisms in pattern-triggered immunity (PTI). *Mol. Plant* **8**, 521–539 (2015).
82. M. C. Rentel *et al.*, OX11 kinase is necessary for oxidative burst-mediated signalling in Arabidopsis. *Nature* **427**, 858–861 (2004).
83. J. Xu *et al.*, A protein kinase, interacting with two calcineurin B-like proteins, regulates K⁺ transporter AKT1 in Arabidopsis. *Cell* **125**, 1347–1360 (2006).
84. T. Yang, S. Chaudhuri, L. Yang, L. Du, B. W. Poovaiah, A calcium/calmodulin-regulated member of the receptor-like kinase family confers cold tolerance in plants. *J. Biol. Chem.* **285**, 7119–7126 (2010).
85. C. Zhao *et al.*, MAP kinase cascades regulate the cold response by modulating ICE1 protein stability. *Dev. Cell* **43**, 618–629.e5 (2017).
86. A. Costa *et al.*, Ca²⁺-dependent phosphoregulation of the plasma membrane Ca²⁺-ATPase ACA8 modulates stimulus-induced calcium signatures. *J. Exp. Bot.* **68**, 3215–3230 (2017).
87. S. Giacometti *et al.*, Phosphorylation of serine residues in the N-terminus modulates the activity of ACA8, a plasma membrane Ca²⁺-ATPase of Arabidopsis thaliana. *J. Exp. Bot.* **63**, 1215–1224 (2012).
88. D. L. Yang *et al.*, Calcium pumps and interacting BON1 protein modulate calcium signature, stomatal closure, and plant immunity. *Plant Physiol.* **175**, 424–437 (2017).
89. S. Rigas *et al.*, TRH1 encodes a potassium transporter required for tip growth in Arabidopsis root hairs. *Plant Cell* **13**, 139–151 (2001).
90. C. Bao *et al.*, Arabidopsis VILLIN2 and VILLIN3 act redundantly in sclerenchyma development via bundling of actin filaments. *Plant J.* **71**, 962–975 (2012).
91. H. S. van der Honing, H. Kieft, A. M. C. Emons, T. Ketelaar, Arabidopsis VILLIN2 and VILLIN3 are required for the generation of thick actin filament bundles and for directional organ growth. *Plant Physiol.* **158**, 1426–1438 (2012).
92. C. C. Hsu *et al.*, Universal plant phosphoproteomics workflow and its application to tomato signaling in response to cold stress. *Mol. Cell. Proteomics* **17**, 2068–2080 (2018).
93. A. B. Iliuk, V. A. Martin, B. M. Alicie, R. L. Geahlen, W. A. Tao, In-depth analyses of kinase-dependent tyrosine phosphoproteomes based on metal ion-functionalized soluble nanopolymers. *Mol. Cell. Proteomics* **9**, 2162–2172 (2010).
94. B. R. T. Dimayacyac-Esleta *et al.*, Rapid high-Ph reverse phase tagetip for sensitive small-scale membrane proteomic profiling. *Anal. Chem.* **87**, 12016–12023 (2015).
95. H. Mi, A. Muruganujan, D. Ebert, X. Huang, P. D. Thomas, PANTHER version 14: More genomes, a new PANTHER GO-slim and improvements in enrichment analysis tools. *Nucleic Acids Res.* **47**: D419–D426 (2019).